

Banner appropriate to article type will appear here in typeset article

On energy-aware hybrid models

Igor Shevchenko¹† and Dan Crisan²

¹National Oceanography Centre, European Way, Southampton, SO14 3ZH, UK

²Department of Mathematics, Imperial College London, 180 Queen's Gate, London, SW7 2AZ, UK

(Received xx; revised xx; accepted xx)

This study proposes deterministic and stochastic energy-aware hybrid models that enable simulations of Geophysical Fluid Dynamics (GFD) models at low resolutions without compromising on quality compared with high-resolution reference runs. Such hybrid models bridge the data-driven and physics-driven modelling paradigms by combining regional stability (the principle underlying the hyper-parameterization approach) and classical GFD models at low resolution that cannot reproduce high-resolution reference flow features (large-scale flows and small-scale vortices) which are, however, resolved. The paradigms are fused through the use of an energy-aware correction of advection velocity and extra forcing compensating for the drift of the low-resolution model away from the reference phase space. The main advantage of hybrid models is that they allow for physics-driven flow recombination within the reference energy band and reproduce resolved reference flow features in low-resolution settings. Hybrid models produce more accurate ensemble predictions than their classical GFD counterparts.

The proposed hybrid approach has been tested on a three-layer quasi-geostrophic (QG) model for a beta-plane Gulf Stream flow configuration. The results show that the low-resolution hybrid QG model reproduces the reference flow features that are resolved on the coarse grid and also gives a more accurate ensemble forecast than the physics-driven QG model.

Hybrid models offer appealing benefits and flexibility to the modelling and forecasting communities, as they are computationally cheap, can use both numerically-computed flows and observations from different sources, require minimalistic interventions into the dynamical core of the underlying model, and produce more accurate ensemble forecasts than classical deterministic GFD models. All these suggest that the hybrid approach has the potential to exploit low-resolution models for long-term climate projections thus offering a new cost effective way of GFD modelling.

1. Introduction

The surge in data-driven modelling has currently influenced the traditional course of Geophysical Fluid Dynamics to split into two branches. One branch continues to use the physics-driven approach based on classical models (e.g. Vallis (2016)), while the other started employing the data-driven approach (e.g. Agarwal *et al.* (2021)). The physics-driven approach is believed to provide more accurate than current future projections at resolutions

† Email address for correspondence: igor.shevchenko@noc.ac.uk

only achievable on at least exascale computers. Although the era of exascale computations is picking up speed in the world, routine long-time exa-simulations and their analysis is still to be achieved, while the need in reliable climate models is urgent given the current climate concerns. On the other hand, data-driven approaches promise faster simulations, while providing a similar level of fidelity to the physics-driven models. Currently, many data-driven approaches exploit artificial neural networks (e.g. Dramsch (2020); Brunton *et al.* (2020)) trained on reference runs of physics-driven models.

In this work we offer a hybrid approach that combines classical models and the data-driven hyper-parameterization (HP) approach (e.g. Shevchenko & Berloff (2021, 2022*a,b*, 2023)). The latter shifts the focus from the physical space to the phase space also known as state space. It considers the inability of the low-resolution model to reproduce resolved reference flow structures as the persistent tendency of the phase space trajectory (the low-resolution solution) to escape the reference phase space (the phase space of the reference solution); *note that the term “low-resolution” in the context of HP approach is relative, and only reflects the fact that the resolution of the HP solution is lower than that of the reference solution.* The philosophy behind the hybrid approach is to augment the classical model at low resolution with reference data in order to ensure that a given measure of goodness holds. In this work, the measure of goodness is that the solution of the hybrid model (or hybrid for short) lies within the reference energy band. It is chosen so that to ensure a long-term evolution of the hybrid on the reference energy manifold and to retain reference flow features that are resolved at low resolution; the reference energy manifold is a hyper-surface (in the phase space) on which the energy of the reference solution has a prescribed energy band. In a nutshell, the hybrid approach rests on the hypothesis that nonlinear interactions in the hybrid model will improve intra- and inter-scale energy transfers towards the reference ones through the control of energy on specific scales.

The strong point of the hybrid approach is that it allows for any physics-driven flow recombination within the reference energy band and reproduces resolved reference flow features. The hybrid approach offers a wide range of advantages and a great flexibility to ocean and atmosphere modellers working with models and observations. Namely, (1) hybrid models are computationally inexpensive (a hybrid run is on the scale of the coarse-grid model simulation); (2) they can use both numerically-computed flows and measurements from different sources (drifters, weather stations, satellites, etc.) as reference data; and (3) require minimalistic interventions into the dynamical core of the underlying model.

2. Hybrid hyper-parameterization models

The hybrid approach assumes that a low-resolution model which cannot reproduce high-resolution reference flow features (which are, however, resolved at low resolution) can be turned into one that is capable of doing so. It is possible to achieve this if (1) the total energy of the hybrid model lies within the reference energy band and (2) the hybrid model respects the regional stability property. We define the latter as a property of the solution of a differential equation

$$\frac{d\mathbf{x}}{dt} = \mathbf{F}(\mathbf{x}), \quad \mathbf{x} \in \mathbb{R}^n \quad (2.1)$$

to permanently remain in a neighborhood of a given region of the phase space if the initial condition is sufficiently close to that region.

The first hybrid HP model has been proposed in (Shevchenko & Berloff 2022*a*). Its dynamical core comprises a quasi-geostrophic (QG) model augmented with the constrained optimization machinery that confines the flow dynamics to evolve with the reference phase

space. The hybrid approach proposed in this study is another step forward towards the use of low-resolution GFD models in long-term climate projections. At the core of the approach lies hybrid models using the following:

- an advection velocity corrector \mathbf{A} ;
- an extra forcing \mathbf{G} compensating the drift of the model away from the reference phase space;
- a multi-scale decomposition \mathbf{M} ;
- an optimization method that searches for spatial scale amplitudes such that the total energy of the hybrid is within the reference band.

For the illustration purposes, we consider the transport equation for a quantity ϕ

$$\partial_t \phi + \mathbf{v} \cdot \nabla \phi = \mathbf{F}(\phi) \quad (2.2)$$

with $\mathbf{v}(t, \cdot)$ being the velocity vector; the dot in the argument of \mathbf{v} means the space dependence. Typically, (2.2) is solved at high resolution, and every run is computationally too intensive to allow for long-term or large ensemble simulations. An affordable option would be a hybrid model that could run at lower resolution on the one hand, while reproducing resolved on the coarse-grid flow features of the reference high-resolution flow dynamics on the other.

We propose the following hybrid model corresponding to (2.2):

$$\partial_t \psi + (\mathbf{u} + \mathbf{A}(\mathbf{u}, \mathbf{v})) \cdot \nabla \psi = \mathbf{F}(\psi) + \mathbf{G}(\psi, \phi), \quad \mathbf{G}(\psi, \phi) := \eta(\mathbf{M}(\psi, \phi) - \psi) \quad (2.3)$$

with η being the nudging strength, and \mathbf{M} is the multi-scale decompositions defined as

$$\mathbf{M}(\psi, \phi) := \sum_{s=1}^S \lambda_s \mathcal{M}_s(\psi, \widehat{\phi}), \quad \widehat{\phi} := \frac{1}{M} \sum_{i=U_t} \mathcal{P}(\phi_i) \Big|_{\mathcal{U}(\psi(t, \cdot))}, \quad (2.4)$$

where $\mathcal{M}_s : \widehat{\phi} \rightarrow \widehat{\phi}_s$ is an operator extracting the s -scale flow dynamics, $\widehat{\phi}_s$, from $\widehat{\phi}$, which includes all (both underresolved and resolved on the computational grid) spatial scales, λ_s is the amplitude of $\widehat{\phi}_s$, S is the total number of scales in the decomposition, \mathcal{P} is a projector from high to low resolution, $\mathcal{U}(\psi(t, \cdot))$ is a neighbourhood of $\psi(t, \cdot)$ in the reference phase space, and U_t is the set of timesteps indexing the discrete reference solution ϕ in the neighbourhood of $\psi(t, \cdot)$. The velocity corrector

$$\mathbf{A}(\mathbf{u}, \mathbf{v}) := \sum_{s=1}^S \gamma_s \mathcal{M}_s(\widehat{\mathbf{v}}), \quad \widehat{\mathbf{v}} := \frac{1}{M} \sum_{i=U_t} \mathcal{P}(\mathbf{v}_i) \Big|_{\mathcal{U}(\psi(t, \cdot))} \quad (2.5)$$

with index i being the same as the one in (2.4). An alternative to the velocity corrector is to consider the following stochastic correction

$$\mathbf{A}(\mathbf{u}, \mathbf{v}) := \sum_{s=1}^S \gamma_s \mathcal{M}_s(\widehat{\mathbf{v}}) dt + \sum_{s=1}^S \mathcal{M}_s(\widehat{\mathbf{v}}) \circ dW_t^s, \quad (2.6)$$

with independent Brownian motions dW_t^s . In this case the hybrid model (2.3) becomes:

$$d\psi + (\mathbf{u} dt + \mathbf{A}(\mathbf{u}, \mathbf{v})) \cdot \nabla \psi = (\mathbf{F}(\psi) + \mathbf{G}(\psi, \phi)) dt. \quad (2.7)$$

The velocity correction (2.6) turns the hybrid model (2.7) into a stochastic hybrid, which is a SALT-class model (Holm 2015). The principle difference with the original SALT approach is that instead of the multi-scale decomposition it uses Empirical Orthogonal Functions which are calibrated on the reference data before the simulation (e.g. (Cotter *et al.* 2019, 2020a,b,c; Crisan *et al.* 2023)). In the hybrid approach, the calibration is performed on the fly (by searching for optimal amplitudes) as the simulation goes on. We will consider both the deterministic and stochastic versions of velocity correction and study how they influence the flow dynamics.

Reference data acquisition. In order to get the reference solution $\{\phi_{i \in [1, N]}\}$ and velocity

$\{\mathbf{v}_{i \in [1, N]}\}$, with N being the number of records, for the hybrid HP model (2.3), we simulate the reference model (2.2) at high resolution and project ϕ and \mathbf{v} onto the grid used in the hybrid model; note that the high-resolution model runs only once (before the hybrid simulation) to acquire reference data, this reference run is assumed to be considerably shorter than that of the hybrid model. If also observations are available, one can project them onto the hybrid model grid and then add them to the reference data set. In this case the reference data set becomes $\{\phi_{i \in [1, N]}, \tilde{\phi}_{j \in [1, M]}\}$ and $\{\mathbf{v}_{i \in [1, N]}, \tilde{\mathbf{v}}_{j \in [1, M]}\}$, where the tilde stands for the observed variable. In case of no numerical simulations available, one can solely use observations. Note that we use the point-to-point projection, but the coarse-graining procedure can be done differently (e.g. by using interpolation schemes, spectral filters, or by spatially averaging the fine-grid solution over the coarse grid cell, etc.)

The multi-scale decomposition controls the amount of energy added to or removed from the hybrid model on a given scale. Operator \mathcal{M}_s can be thought of as a spatial filter or an evolutionary model computing the s -scale flow $\tilde{\phi}_s$. We use the spectral filtering (e.g. Sagaut (2006)), but the choice is not limited to the one, and can be chosen based on the problem-dependent requirements.

The neighborhood $\mathcal{U}(\psi(t, \cdot))$ is calculated as the average over M nearest, in l_2 -norm, to the hybrid solution $\psi(t, \cdot)$ points in the reference phase space, i.e. in the phase space of model (2.2). For all simulations presented below, we take $M = 10$ (as in the first HP method (Shevchenko & Berloff 2021)) and note that this parameter is of minor importance, as the optimization method delivers amplitudes λ_s and γ_s to ensure the energy of the hybrid model is within the reference energy band.

The number of spatial scales S is calculated based on what the hybrid model can resolve and what it can not. We use a 2-scale decomposition ($S = 2$), which splits the flow into two: the first one includes all underresolved scales, while the second includes all resolved scales. A more general approach would be to compare the total energy of the reference model at high and low resolutions, and decompose the flow into scales the energy on which need correction.

Energy calculation. In order to keep the total energy of the hybrid model within the reference energy band, we compute kinetic and potential energies. If potential energy is not available then one should use only the kinetic energy which is typically a standard diagnostic in ocean and atmospheric models. Note that it is more efficient to calculate the energies for all reference data before running the hybrid model, as it allows to avoid unnecessary recomputations of energy during the simulation.

Optimization method. The last ingredient of the hybrid approach is the optimization method. We use Powell's method (Powell 1964) which is a derivative free optimization method, and avoid methods computing gradients, as it is an unnecessary complication for this study. Note that the nudging strength η can also be included in the optimization, but we keep it constant at 0.02 in this work and optimize for scale amplitudes λ_s and γ_s such that for $\forall t \geq 0$ one of the following criteria holds:

$$(C1) \quad \|\bar{E} - E(\psi(t, \cdot))\|_2 \leq \varepsilon \quad (2.8a)$$

$$(C2) \quad \|E(\hat{\phi}) - E(\psi(t, \cdot))\|_2 \leq \varepsilon \quad (2.8b)$$

with ε being a tolerance (in this study $\varepsilon = 10^{-6}$).

The optimization method can significantly affect not only the accuracy but also the performance of the hybrid approach. Namely, the orbital search for optimal amplitudes along long trajectories can take a considerable toll on the overall performance, because it optimizes for amplitudes to ensure that starting from an initial condition $\psi(t_i, \cdot)$ one of the optimization criteria is satisfied for $\psi(t_j, \cdot)$, $j \gg i$. Therefore, one should find the right

balance between performance and accuracy for a given problem. We optimize in the last time step every 24 hours; the time step is 0.5 hour. As an alternative, one can engage the orbital search over the 24-hour trajectory. We have tried the latter too, but did not observe any improvement compared to the former.

3. Multilayer quasi-geostrophic model

In this section we apply the hybrid approach to the three-layer quasi-geostrophic (QG) model for the evolution of potential vorticity (PV) anomaly $\mathbf{q} = (q_1, q_2, q_3)$ (Pedlosky 1987):

$$\partial_t q_j + \mathbf{v}_j \cdot \nabla q_j = F, \quad F := \delta_{1j} F_w - \delta_{j3} \mu \nabla^2 \psi_j + \nu \nabla^4 \psi_j - \beta \psi_{jx}, \quad j = 1, 2, 3, \quad (3.1)$$

with $\psi = (\psi_1, \psi_2, \psi_3)$ being the velocity streamfunction, δ_{ij} is the Kronecker symbol, and \mathbf{v} is the velocity vector; the planetary vorticity gradient is $\beta = 2 \times 10^{-11} \text{ m}^{-1} \text{ s}^{-1}$, the bottom friction is $\mu = 4 \times 10^{-8} \text{ s}^{-1}$, and the lateral eddy viscosity is $\nu = 50 \text{ m}^2 \text{ s}^{-1}$. The asymmetric wind curl forcing, driving the double-gyre ocean circulation, is given by

$$F_w = \begin{cases} -1.80 \pi \tau_0 \sin(\pi y / y_0), & y \in [0, y_0), \\ 2.22 \pi \tau_0 \sin(\pi(y - y_0) / (L - y_0)), & y \in [y_0, L], \end{cases}$$

with the wind stress amplitude $\tau_0 = 0.03 \text{ N m}^{-2}$ and the tilted zero forcing line $y_0 = 0.4L + 0.2x$, $x \in [0, L]$. The computational domain $\Omega = [0, L] \times [0, L] \times [0, H]$ is a closed, flat-bottom basin with $L = 3840 \text{ km}$, and the total depth $H = H_1 + H_2 + H_3$ given by the isopycnal fluid layers of depths (top to bottom): $H_1 = 0.25 \text{ km}$, $H_2 = 0.75 \text{ km}$, $H_3 = 3.0 \text{ km}$.

The PV anomaly \mathbf{q} and the velocity streamfunction ψ are coupled through the system of elliptic equations:

$$\mathbf{q} = \nabla^2 \psi - \mathbf{S} \psi, \quad (3.2)$$

with the stratification matrix

$$\mathbf{S} = \begin{pmatrix} 1.19 \cdot 10^{-3} & -1.19 \cdot 10^{-3} & 0.0 \\ -3.95 \cdot 10^{-4} & 1.14 \cdot 10^{-3} & -7.47 \cdot 10^{-4} \\ 0.0 & -1.87 \cdot 10^{-4} & 1.87 \cdot 10^{-4} \end{pmatrix}.$$

The stratification parameters are given in units of km^{-2} and chosen so that the first and second Rossby deformation radii are $Rd_1 = 40 \text{ km}$ and $Rd_2 = 23 \text{ km}$, respectively; the choice of these parameters is typical for the North Atlantic, as it allows to simulate a more realistic (than in different QG setups) but yet idealized eastward jet extension of the western boundary currents.

System (3.1)-(3.2) is augmented with the mass conservation constraint (McWilliams 1977):

$$\partial_t \iint_{\Omega} (\psi_j - \psi_{j+1}) dy dx = 0, \quad j = 1, 2 \quad (3.3)$$

with a zero initial condition and a partial-slip boundary condition (Haidvogel *et al.* 1992):

$$\left(\partial_{\mathbf{nn}} \psi - \alpha^{-1} \partial_{\mathbf{n}} \psi \right) \Big|_{\partial\Omega} = 0, \quad (3.4)$$

where $\alpha = 120 \text{ km}$ is the partial-slip parameter, and \mathbf{n} is the normal-to-wall unit vector.

Before proceeding to the hybrid QG model, we explain how to compute the reference data $\{\mathbf{q}_i, \mathbf{v}_i\}_{i \in [1, N]}$. In order to generate it, we first spin up the QG model for 50 years on a high-resolution grid of size 513×513 (grid step is $dx = dy = 7.5 \text{ km}$) until the solution is statistically-equilibrated on the energy manifold (figure 1), we then run the model for another 2 years, and point-to-point project the 2-year solution onto the coarse grid of size 129×129

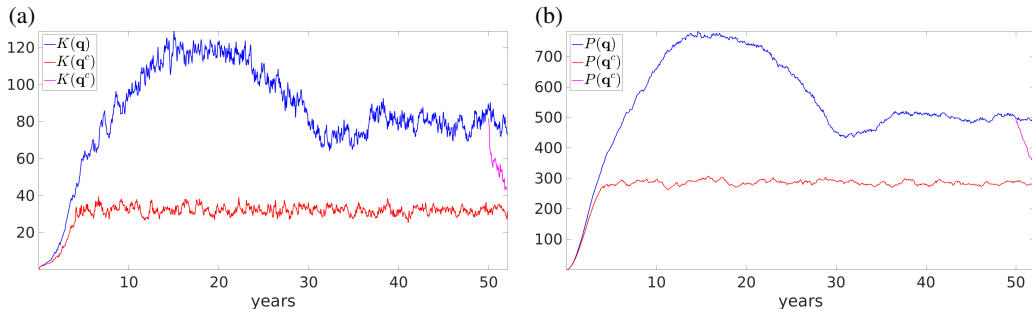


Figure 1: Time series of the non-dimensional (a) kinetic and (b) potential energies for the reference \mathbf{q} (blue) and low-resolution \mathbf{q}^c (red) solutions over the interval of 52 years. We also show the energies of the low-resolution solution started from the reference initial condition after the spinup (magenta). These energies undergo a rapid and significant drop compared with the reference energy level.

(grid step is $dx = dy = 30$ km). Finally, we take only the first year as the reference solution, and keep the second year for validation of the hybrid model.

As seen in figure 1, over the first approximately 38 years the reference solution \mathbf{q} is in transit showing significant variations of kinetic $K(\mathbf{q})$ and potential, $P(\mathbf{q})$, energies; the low-resolution solution \mathbf{q}^c (computed on the coarse grid) is equilibrated much faster though. The striking difference between these solutions is that $K(\mathbf{q}^c)$ and $P(\mathbf{q}^c)$ are significantly lower than $K(\mathbf{q})$ and $P(\mathbf{q})$. More importantly, $K(\mathbf{q}^c)$ and $P(\mathbf{q}^c)$ experience a sudden fall compared with $K(\mathbf{q})$ and $P(\mathbf{q})$, when started from a reference initial condition after the spinup. Eventually, both $K(\mathbf{q}^c)$ and $P(\mathbf{q}^c)$ reach even lower levels, which are natural to the low-resolution solution. This is typical and explained by the significant energy dissipation in the coarse-grid model and its impaired intra- and inter-scale energy transfers (including both forward and backward energy cascades). In phase space, this energy drop is observed as a drift of the low-resolution trajectory (solution) from the reference phase space, because the trajectory is gradually slipping off from the reference energy manifold.

4. The hybrid quasi-geostrophic model

In order to get the hybrid QG model, we add the velocity corrector \mathbf{A} and the compensating forcing \mathbf{G} to the QG model (3.1):

$$dq_j^h + (\mathbf{v}_j^h dt + \mathbf{A}(\mathbf{v}_j^h, \mathbf{v}_j)) \cdot \nabla q_j^h = (F + \mathbf{G}(q_j^h, q_j)) dt, \quad (4.1)$$

where $\mathbf{G}(q_j^h, q_j) := \eta(\mathbf{M}(q_j^h, q_j) - q_j^h)$, and the superscript h denotes the hybrid solution. The system of elliptic equations (3.2), the mass conservation constraint (3.3), and the boundary condition (3.4) remain unchanged.

In order to study how velocity correction and compensating forcing influences the flow dynamics and energy, it is important to consider three deterministic cases with \mathbf{A} defined by (2.5): (i) $\mathbf{A} = 0$ and $\mathbf{G} \neq 0$; (ii) $\mathbf{A} \neq 0$ and $\mathbf{G} = 0$; (iii) $\mathbf{A} \neq 0$ and $\mathbf{G} \neq 0$; and (iv) stochastic case of (iii) with \mathbf{A} defined by (2.6).

Deterministic case ($\mathbf{A} = 0$ and $\mathbf{G} \neq 0$). To start with this case, we perform the multi-scale decomposition of the reference data $\{\mathbf{q}_i, \mathbf{v}_i\}_{i \in [1, N]}$. For the purpose of this study, it is enough to decompose the reference data into two fields: the first one includes all scales within the range $s_1 \in [30, 300]$ km, and the second one includes all scales within the range $s_2 \in [300, 3840]$ km. It is done so, because the coarse-grid properly resolves scales larger than 300 km. However, this might be not enough for other GFD models, as an accurate

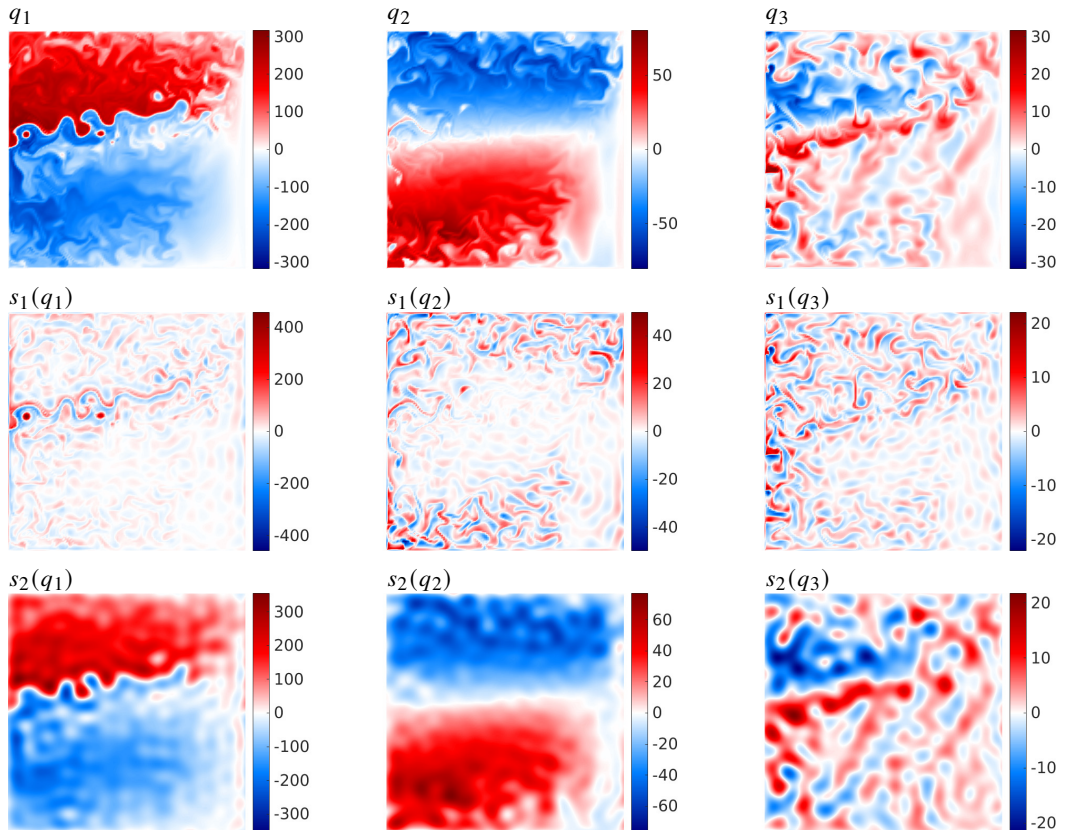


Figure 2: Shown is a typical snapshot of the reference solution \mathbf{q} on different levels, and its multi-scale decomposition into scales $s_1 \in [30, 300]$ km and $s_2 \in [300, 3840]$ km.

resolution of certain scales does not guarantee the proper operation of intra- and inter-scale energy transfers, and therefore more scales should be taken into account.

We present the results of the multi-scale decomposition for both the reference (figure 2) and low-resolution (figure 3) solutions to show how the lack of energy in the coarse-grid model influences the flow dynamics. As seen in figure 3, the coarse-grid model cannot reproduce the idealized Gulf Stream flow and the eddy-gensis is compromised, i.e. there are no eddies observed in the low-resolution solution.

The next step of the hybrid approach is to calculate the reference energy band for the kinetic and potential energies (from the 1-year reference record), which is $K(\mathbf{q}) \in [76, 90]$ and $P(\mathbf{q}) \in [487, 499]$, respectively. These boundaries are used in the optimization method to search for the scale amplitudes.

Given the reference data, its multi-scale decomposition, and the reference energy band, we run the hybrid QG model (4.1) for a period of two years, and use only the first year of the reference data. For the purpose of this study, it is enough to consider the surface layer, as it is much more energetic than the lower layers and full of both large- and small-scale flow features.

We will also consider different ideas on how to maintain the energy of the hybrid model within the reference energy band. Even though some failed, we think it is important for the reader to be aware of these failures to avoid them in the future. The first one is to use the

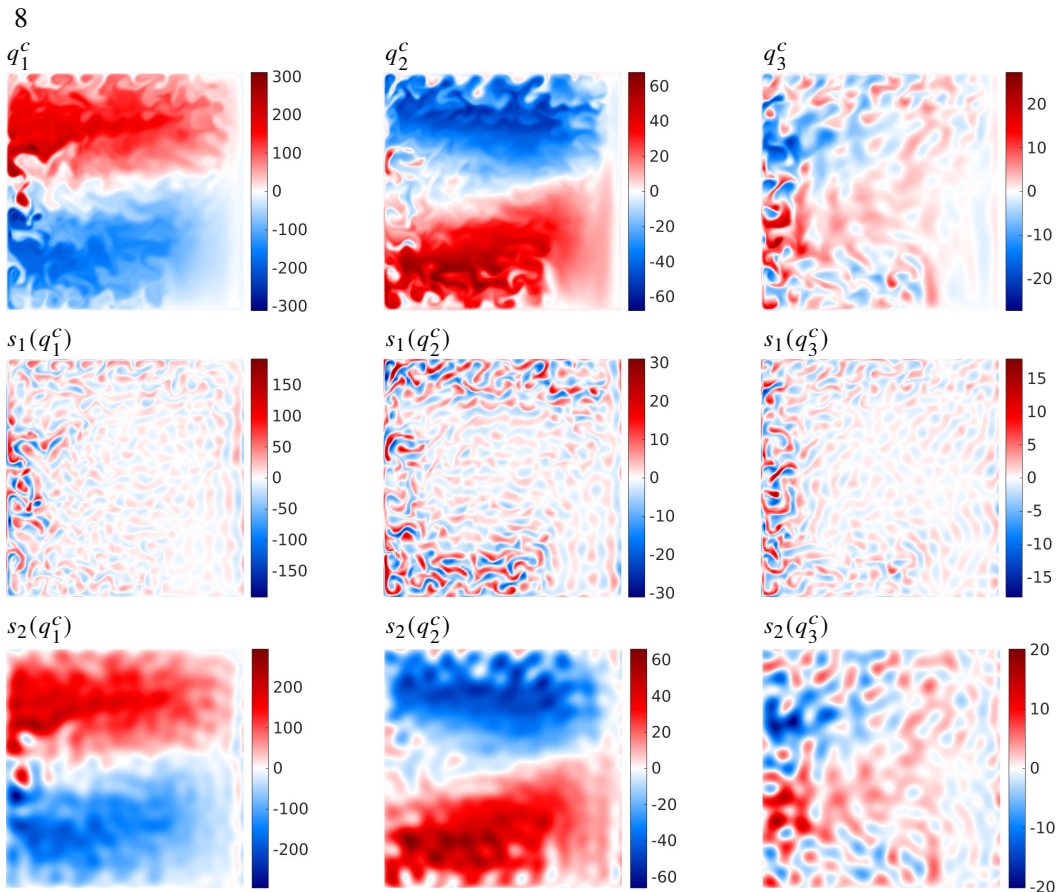


Figure 3: The same as in figure 2 but for the low-resolution solution \mathbf{q}^c .

HP-like nudging (Shevchenko & Berloff 2021) instead of the multi-scale forcing (2.4):

$$\mathbf{G}^*(\mathbf{q}^h, \mathbf{q}) := \eta(\widehat{\mathbf{q}} - \mathbf{q}^h), \quad \widehat{\mathbf{q}} := \frac{1}{M} \sum_{i=U_t} \mathcal{P}(\mathbf{q}_i) \Big|_{U(\mathbf{q}^h(t, \cdot))}, \quad (4.2)$$

which is equivalent to injecting or dissipating energy on all scales, as there is no multi-scale decomposition in use.

The detrimental effect of what happens to the kinetic and potential energies of the hybrid solution (figure 4) and what it does to the flow dynamics (figure 5) is clearly seen. The energy drop in the hybrid and low-resolution models is accompanied by the degradation of eddy activity that in turn results in the inhibition of the Gulf Stream flow. A similar situation (not shown) is observed for the case of fixed amplitudes λ_s computed as the ratio between the time mean energies of the reference and low-resolution solutions on scales $s_1 \in [30, 300]$ km and $s_2 \in [300, 3840]$ km.

Next, we consider how the first optimization criterion (2.8a) affects the energy and flow dynamics. As the results show (figures 6(a,b), magenta graph), it brings the potential energy of the hybrid solution within the reference band, but the kinetic energy is still outside. Moreover, both energies experience high-frequency fluctuations due to constant (and significant) adjustments of the trajectory to satisfy the criterion. It means that the hybrid model is always trying to escape the reference energy manifold because the first criterion does not seem to properly correct intra- and inter-scale energy transfers towards the reference ones,

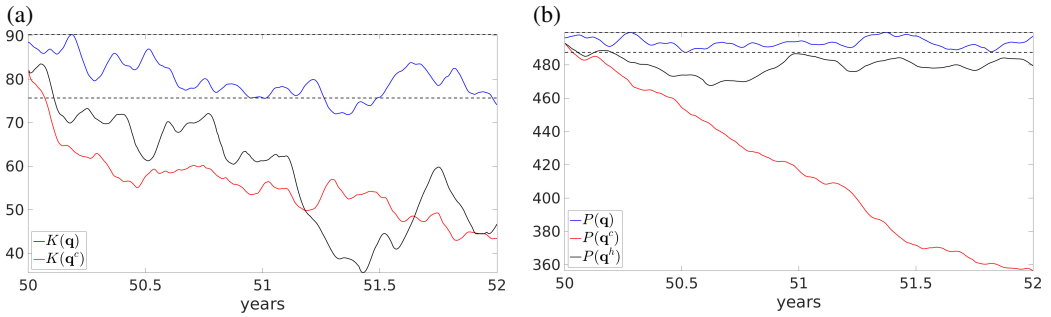


Figure 4: Time series of the non-dimensional (a) kinetic and (b) potential energies of the reference \mathbf{q} (blue), low-resolution solution \mathbf{q}^c (red), and hybrid solution \mathbf{q}^h (black) for the case of using \mathbf{G}^* . The kinetic and potential energies of the hybrid solution rapidly drop below the reference level (dashed line), and even worse – the former decreases lower than that of the low-resolution solution.

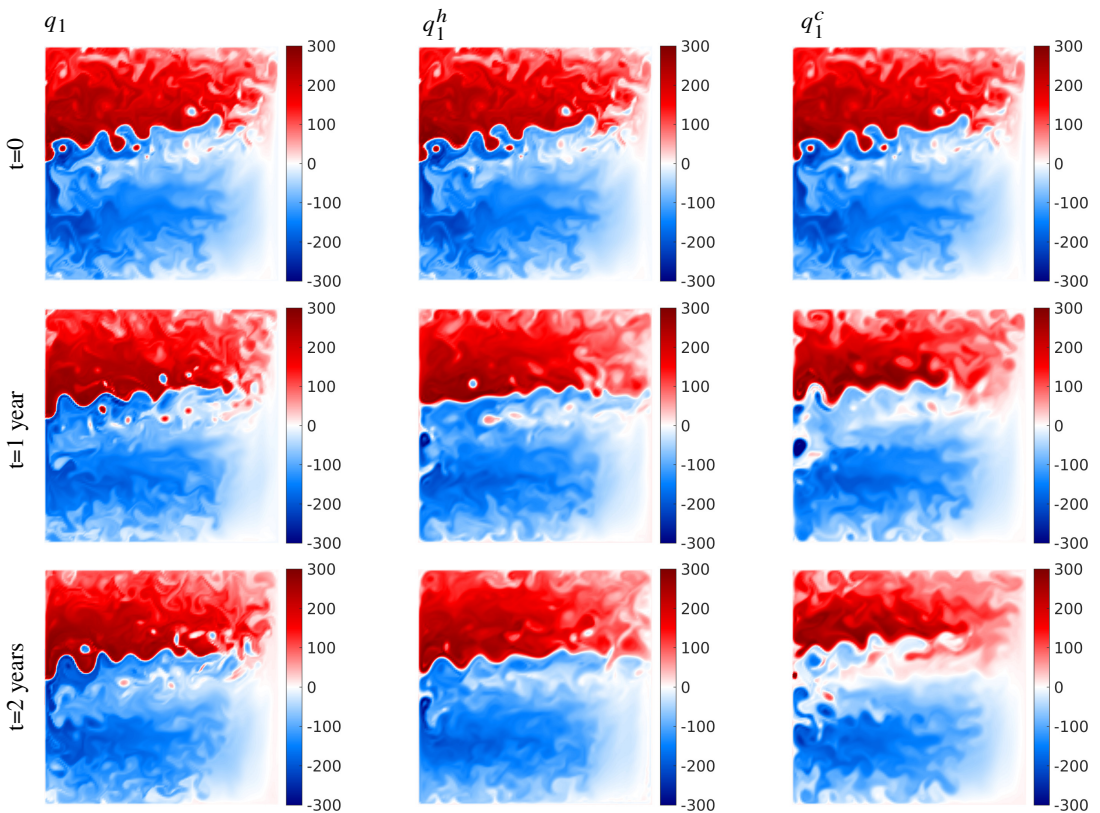


Figure 5: Shown are snapshots of the reference solution q_1 , hybrid solution q_1^h , and low-resolution solution q_1^c at $t = \{0.0, 1.0, 2.0\}$ years. The lack of energy in the hybrid and low-resolution models lead to the loss of eddies and as a result to weakening the Gulf Stream flow.

which in turn leads to significant distortions of the flow dynamics (figure 6(c)). However, the flow dynamics improves dramatically if we use the second criterion (2.8b) (figure 6(d)). Namely, the Gulf Stream flow becomes well-pronounced and teams with vortices, and both the kinetic and potential energies of the hybrid solution are within the reference energy band, although over a short time interval the potential energy experiences a burst out of the

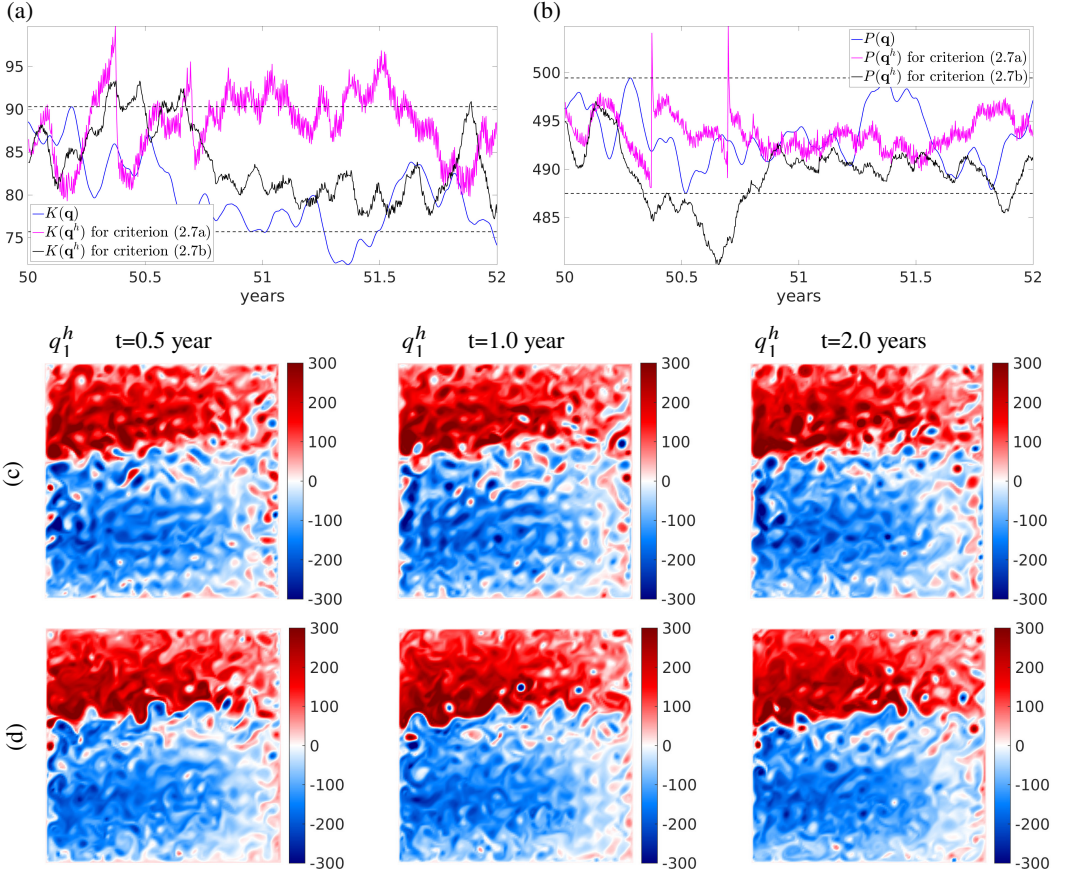


Figure 6: Time series of the non-dimensional (a) kinetic and (b) potential energies of the reference \mathbf{q} (blue), and hybrid solution \mathbf{q}^h for the first criterion (2.8a) (magenta) and for the second criterion (2.8b) (black). The use of the first criterion leads to appearing a high-frequency component in the kinetic and potential energies of the hybrid solution. Moreover, the kinetic energy is above the reference level (dashed line) thus resulting in the abundance of eddies and a less pronounced Gulf Stream flow (c). However, when the second criterion is in use, both the kinetic and potential energies of the hybrid solution are harmonized to the reference levels that results in significant improvements of the hybrid solution towards the reference flow (d).

reference energy manifold. It happens because the optimization method cannot deliver the optimum after a fixed number of iterations used in this study, which is 10.

Deterministic case ($\mathbf{A} \neq 0$ and $\mathbf{G} = 0$). When the compensating forcing is disabled ($\mathbf{G} = 0$), the optimization procedure is unable to keep the energy of the hybrid model within the reference band thus leading to significant releases of energy outside of the reference energy manifold (figures 7(a,b), black graph) that, in turn, leads to significant distortions to the jet itself (figures 7(c)).

Deterministic case ($\mathbf{A} \neq 0$ and $\mathbf{G} \neq 0$). The situation changes rapidly for the better if the compensating forcing is allowed. Namely, the energy of the hybrid model evolves in the reference energy band (figures 7(a,b), green graph) and the flow dynamics shows no sign of jet or vortices degradation (figure 7(d)).

Stochastic case ($\mathbf{A} \neq 0$ and $\mathbf{G} \neq 0$). The stochastic correction results in even more accurate energy representation (figures 7(a,b), orange graph), although the flow dynamics does not show qualitative differences compared to the deterministic case (iii) (figure 7(e)). All in all, the proposed hybrid approach augmented with a stochastic correction of advection

velocity and scale-aware energy control through the compensating forcing improves the intra- and inter-scale energy transfers towards the reference ones thus leading to the low-resolution flow dynamics that reproduces resolved flow features of the reference solution. Moreover, the hybrid approach also respects the regional stability property by keeping the hybrid solution in the vicinity of the reference phase space.

Stochastic ensemble simulations. In this section we focus on stochastic ensembles to compare prediction skills of the hybrid model with its classical GFD counterpart. We consider a 50-member ensemble and run it over a two-month period. We choose this setup as it is similar to those used by the European Centre for Medium-Range Weather Forecasts (ECMWF) for extended-range forecasts. In order to avoid an influence of the reference data, we compare the ensemble over the second validation year (where the reference data is unavailable), and also present the results over the reference year (where the reference data is available) for comparison. Every ensemble member of the hybrid model (4.1) starts from a perturbed reference initial condition. The QG model (3.1) starts from its own initial condition after the spinup, because starting it from the reference initial condition is not allowed as it might give the model an advantage over the drift time (the time the model drifts away from the reference energy manifold until it is equilibrated onto its own lower-energy manifold). It takes around 5 years to equilibrate (not shown). The hybrid model has no drift (or more accurately, its drift is corrected), as its evolution is bounded to the reference energy manifold, and the ensemble start from perturbed reference conditions is therefore justified. However, if the hybrid model starts from an initial condition used for the QG model, then it takes approximately one month for the solution to drift from the low-energy manifold of the QG model to the high-energy reference manifold (not shown). This drift can be significantly accelerated by increasing the nudging strength.

The results are presented in figure 8 in terms of relative bias (RB)

$$RB(\mathbf{q}, \mathbf{q}^h) := \frac{\|\mathbf{q} - \bar{\mathbf{q}}^h\|_2}{\|\mathbf{q}\|_2}, \quad \bar{\mathbf{q}}^h := \frac{1}{N} \sum_{i=1}^N \mathbf{q}_i^h, \quad (4.3)$$

$$\langle RB(\mathbf{q}, \mathbf{q}^h) \rangle := \frac{1}{6} \sum_{i=0}^5 RB(\mathbf{q}_{[2i, 2(i+1)]}, \mathbf{q}_{[0, 2]}^h),$$

and l_2 -norm relative error (RE):

$$RE(\mathbf{q}, \mathbf{q}^c) := \frac{\|\mathbf{q} - \mathbf{q}^c\|_2}{\|\mathbf{q}\|_2}, \quad (4.4)$$

with $N = 50$. The 2-month relative bias RB is averaged over one year, which is not included in the reference dataset.

As seen in figure 8, the ensemble forecast of the hybrid is more accurate than that of the QG model (3.1). Moreover, this forecast is systematically better not only over two months, but over the whole validation year. It demonstrates the potential of the hybrid model to produce reliable forecast well beyond the reference dataset. The short fluctuation of the relative bias over the first ~ 24 hours into the simulation is due to the adjustment of the hybrid model to the reference energy manifold. It happens as the perturbation of the reference initial condition can be outside of the reference energy band. The saw-like behaviour of the relative bias is due to the correction of the hybrid solution towards the reference energy manifold.

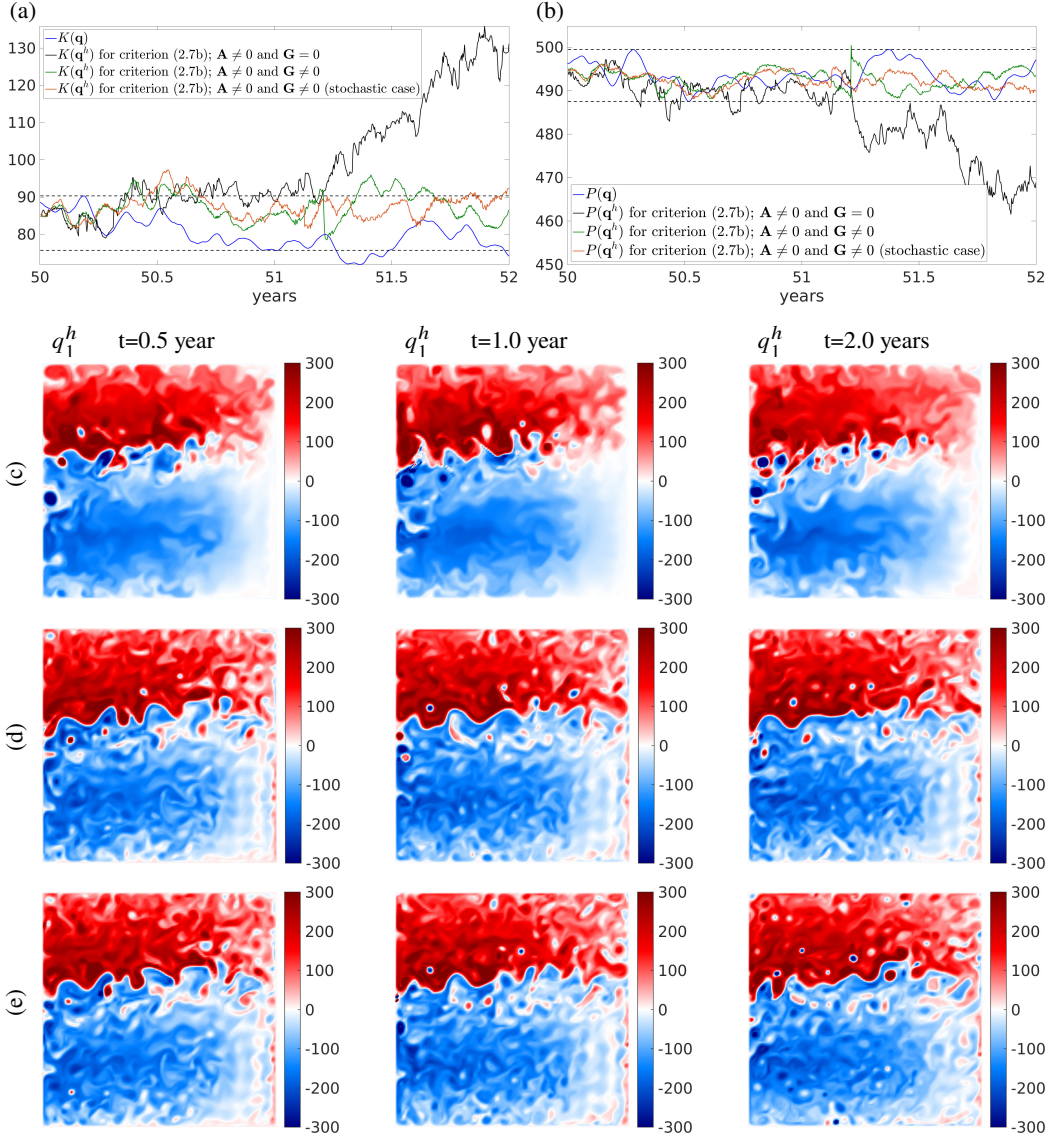


Figure 7: Time series of the non-dimensional (a) kinetic and (b) potential energies of the reference q (blue), and hybrid solution q^h for the second criterion (2.8b): case (ii) $A \neq 0$ and $G = 0$ (black); (iii) $A \neq 0$ and $G \neq 0$ (green); and case (iv) stochastic version of case (iii) (orange). For case (ii), when the compensating forcing is disabled, both kinetic and potential energy is well beyond the reference energy band which results in a significant corruption of the Gulf Stream flow along the jet (c). For case (iii), when the compensating forcing is enabled, the kinetic and potential energies (green) are within the reference energy band, and the Gulf Stream flow dynamics is improved towards the reference one (d). For case (iv), when the stochastic version of the velocity corrector A is used together with the compensating forcing G , the kinetic and potential energies (orange) are even more accurate compared to all other cases, although the flow dynamics (e) does not manifest qualitative differences compared to case (iii).

5. Conclusions and discussion

In this study we have proposed a hybrid approach based on deterministic and stochastic energy-aware hybrid models that combine the principle of regional stability used in the hyper-

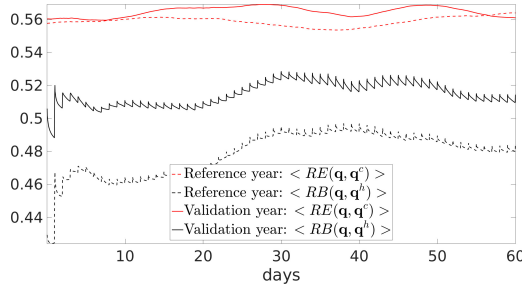


Figure 8: Shown is the relative bias (black) and l_2 -norm relative error (red) over a 2-month period, averaged over one year. The results are presented for the reference year (dashed line) over which the reference data is available and validation year (solid line) over which the reference data is not available. The results clearly show that the hybrid ensemble forecast is more accurate than that of the QG model over the validation year. The results for the reference year are given for comparison.

parameterization approach and classical GFD models at low resolution that cannot reproduce high-resolution reference flow features which are, however, resolved at low resolution. The hybrid approach utilizes the velocity correction and energy-aware forcing (compensating for the tendency of the classical model to leave the reference energy manifold) in order to improve intra- and inter-scale energy transfers towards the reference ones through the control of energy on specific scales.

We have tested the hybrid approach on the three-layer QG model and studied how different forcing terms affect its energy and flow dynamics. We have found that the forcing based on the HP-like nudging and constant scale amplitudes does not improve the hybrid solution towards the reference one, as the hybrid solution energies are outside of the reference energy band. The first optimization criterion improves the situation but the energy of the hybrid model becomes contaminated with high-frequencies (resulting from constant corrections of the trajectory towards the reference phase space) which are not present in the reference solution. The forcing using the second optimization criterion significantly improves the hybrid solution so that it reproduces resolved on the coarse grid features of the reference flow. This improvement is achieved through keeping the kinetic and potential energies of the hybrid solution on the reference energy manifold and through respecting the regional stability.

In studying the deterministic and stochastic hybrid QG models we have found that the stochastic model provides a marginally more accurate representation of the energy compared to the deterministic model, while the flow dynamics is qualitatively the same for both models. However, the stochastic model allows to produce ensembles which are systematically more accurate than the solution of the deterministic QG model as well as to apply a data assimilation methodology based on ensemble particle filters which we will consider in a sequel to this paper.

The main advantage of the hybrid approach is that it allows for any physics-driven flow recombination within the reference energy band and reproduces resolved reference flow features in low-resolution models. Hybrid models offer appealing benefits and flexibility to GFD modellers and the forecasting community, as (1) they are computationally cheap (a hybrid run is on the scale of the coarse-grid model simulation); (2) can use both numerically-computed flows and observations; (3) require minimalistic interventions into to the dynamical core of the underlying model, only the advection velocity is corrected and one term is added to the right hand side; (4) produce more accurate ensemble forecasts than classical GFD models.

The ability of energy-aware stochastic hybrid model to provide high-quality solutions

(given the fact that the computational cost of hybrid runs is that of the low-resolution ocean model with modest overhead) allows for the use of larger ensembles and longer forecast horizons compared with the reference runs. The hybrid approach offers a great resolution scalability and can be used to parametrise the effect of any high-resolution process into lower-resolution systems (e.g. mesoscale processes in larger-scale processes, sub-mesoscale processes in mesoscale-resolving, etc.), and therefore it can be readily adopted by forecasting systems to increase the resolution of the resolved dynamics.

We conclude that the hybrid approach has the potential to be used for long-term climate projections with low-resolution GFD models, which are currently not capable of playing this role.

Acknowledgements.

Funding. Igor Shevchenko thanks the Natural Environment Research Council for the support of this work through the projects CLASS and ATLANTIS. Dan Crisan thanks the European Research Council (ERC) under the European Union’s Horizon 2020 Research and Innovation Programme for the partial support of this work through ERC, Grant Agreement No 856408.

Declaration of interests. The authors report no conflict of interest.

REFERENCES

- AGARWAL, N., KONDRASHOV, D., DUEBEN, P., RYZHOV, E. & BERLOFF, P. 2021 A comparison of data-driven approaches to build low-dimensional ocean models. *JAMES* **13**, e2021MS002537.
- BRUNTON, S., NOACK, B. & KOUMOUTSAKOS, P. 2020 Machine learning for fluid mechanics. *Annu. Rev. Fluid Mech.* **52**, 477–508.
- COTTER, C., CRISAN, D., HOLM, D., PAN, W. & SHEVCHENKO, I. 2019 Numerically modelling stochastic Lie transport in fluid dynamics. *Multiscale Model. Simul.* **17**, 192–232.
- COTTER, C., CRISAN, D., HOLM, D., PAN, W. & SHEVCHENKO, I. 2020a A Particle Filter for Stochastic Advection by Lie Transport (SALT): A case study for the damped and forced incompressible 2D Euler equation. *SIAM/ASA Journal on Uncertainty Quantification* Accepted.
- COTTER, C., CRISAN, D., HOLM, D., PAN, W. & SHEVCHENKO, I. 2020b Data assimilation for a quasi-geostrophic model with circulation-preserving stochastic transport noise. *Journal of Statistical Physics* **179**, 1186–1221.
- COTTER, C., CRISAN, D., HOLM, D., PAN, W. & SHEVCHENKO, I. 2020c Modelling uncertainty using stochastic transport noise in a 2-layer quasi-geostrophic model. *Foundations of Data Science* **2**, 173–205.
- CRISAN, D., LANG, O., LOBBE, A., VAN LEEUWEN, PETER-JAN & POTTHAST, R. 2023 Noise calibration for SPDEs: A case study for the rotating shallow water model. *Foundations of Data Science* .
- DRAMSCH, J. 2020 Chapter one - 70 years of machine learning in geoscience in review. *Adv. Geophys.* **61**, 1–55.
- HAIDVOGEL, D., MCWILLIAMS, J. & GENT, P. 1992 Boundary current separation in a quasigeostrophic, eddy-resolving ocean circulation model. *J. Phys. Oceanogr.* **22**, 882 – 902.
- HOLM, D. 2015 Variational principles for stochastic fluids. *Proc. Roy. Soc. A* **471**.
- MCWILLIAMS, J. 1977 A note on a consistent quasigeostrophic model in a multiply connected domain. *Dynam. Atmos. Ocean* **5**, 427–441.
- PEDLOSKY, J. 1987 *Geophysical fluid dynamics*. Springer-Verlag, New York.
- POWELL, M 1964 An efficient method for finding the minimum of a function of several variables without calculating derivatives. *Comput. J.* **7**, 155–162.
- SAGAUT, P. 2006 *Large eddy Simulation for Incompressible Flows: An Introduction*. Springer Science & Business Media.
- SHEVCHENKO, I. & BERLOFF, P. 2021 A method for preserving large-scale flow patterns in low-resolution ocean simulations. *Ocean Model.* **161**, 101795.
- SHEVCHENKO, I. & BERLOFF, P. 2022a A method for preserving nominally-resolved flow patterns in low-resolution ocean simulations: Constrained dynamics. *Ocean Model.* **178**, 102098.
- SHEVCHENKO, I. & BERLOFF, P. 2022b A method for preserving nominally-resolved flow patterns in low-resolution ocean simulations: Dynamical system reconstruction. *Ocean Model.* **170**, 101939.

- SHEVCHENKO, I. & BERLOFF, P. 2023 A hyper-parameterization method for comprehensive ocean models: Advection of the image point. *Ocean Model.* **184**, 102208.
- VALLIS, G. 2016 Geophysical fluid dynamics: whence, whither and why? *Proc. R. Soc. A.* **472**, 20160140.